“Copenhagen Offshore Wind 2005”

The Effect of Wave Modelling on Offshore Wind Turbine Fatigue Loads

Jenny M. V. Trumars
Chalmers University of Technology
Water Environment Transport
S 412 96 Göteborg, Sweden
Tel: +46 31 772 2149
Fax: +46 31 772 5695
jenny.trumars@wet.chalmers.se

Niels Jacob Tarp-Johansen
Risø National Laboratory
Wind Energy Department, VEA-118
P.O. Box 49
DK-4000 Roskilde, Denmark
Tel: +45 4677 5078
Fax: +45 4677 5960
niels.jacob.tarp-johansen@risoe.dk

Thomas Krogh
Risø National Laboratory
Wind Energy Department, VEA-118
P.O. Box 49
DK-4000 Roskilde, Denmark
Tel: +45 4677 5062
Fax: +45 4677 5960
thomas.krogh@risoe.dk

Topic: Offshore Technology for Wind Energy Application, Design basis – what is required?
Keywords: Non-linear Waves, Wave Load, Wind Energy Converter, Fatigue

ABSTRACT

Due to the pronounced dynamic behaviour of wind turbines, fatigue load effects may be quite sensitive to the precise modelling of the frequency content of the wave loading. As the offshore wind turbine technology progresses, larger and larger turbines will be placed at still deeper waters causing the resonant frequency of the first eigen mode of a traditional bottom-fixed support structure to be typically in the range from 0.25 Hz to 0.35 Hz. As an example wave measurements from the offshore wind farm Bockstigen show a second peak at approximately 0.3 Hz in the wave spectrum. Thus this peak, or similar peaks realized at shallow water sites, may very well be dynamically amplified in the response. This second peak cannot be modelled with a linear wave model and a wave model taking non-linearities into account has to be used. In the presented work both a linear and a non-linear wave model are used to study the fatigue in an offshore wind power plant and the difference is investigated. For the wave modelling two approaches to the calculation of the velocities to the free surface are made. The first being a Taylor extrapolation above the still water level and the second is the use of Wheeler stretching. Time series of irregular linear and non-linear waves are calculated and structural calculations of an offshore wind turbine with a slender support structure are used in the analysis of the fatigue loads. The forces on the structure are calculated using Morison's equation integrating along the structure and lumping the loads in nodes for the structural calculations. From the results it can be concluded that the difference between the wave-models is significant and the non-linear model yields higher fatigue damage than the linear one. It can also be seen that the use of Wheeler stretching yields lower fatigue damage than the use of the Taylor extrapolation.

INTRODUCTION

As energy production from wind power becomes more common, the lack of sites for wind power farms on land is turning into a problem. This has led to an expansion offshore at sites with depths ranging from approximately 6 to 30 m. The expansion at sea is also motivated by better wind conditions and reduced visual disturbance. However, change of location from land to sea changes the design requirements of wind turbines. In addition to wind loads, the wave load on the structure has to be taken into account. To calculate the wave load at the depths in question, a theory for waves at finite depth has to be used.

The chosen wave model is a realization of the sea surface and the velocity potential from a variance density spectrum. The realization is based on the fact that the sea surface elevation and the velocity potential can be calculated by the use of Fourier sums. The velocity is then calculated as the spatial derivative of the velocity potential. The numerical derivative of the velocity with respect to time gives the acceleration, which together with Morison's equation gives the resulting structural loading.

The integrity of a structure is dependent on the fatigue of the structure and on the ultimate loading of the structure. As the wave model used is weakly non-linear, it is not suitable for calculating extreme waves, nor extreme wave loads. There are other models more suitable for that purpose.

The support structure of the considered model wind turbine is a tower mounted on a cylindrical steel monopile piled into the soil and extending above the water surface. The cylinder diameter is 6 m at still water level, and the mean water depth is 20 m at the site. See Fig. 1.

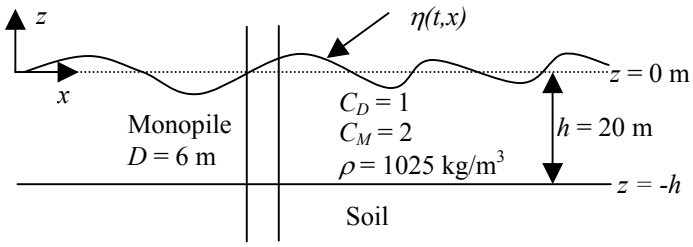

Figure 1. *Details of the monopile. The monopile extends above the sea surface and the water depth is 20 meters. η is the instantaneous free water surface and the dotted line is the still water level.*

The problem of waves on offshore wind power plants has been addressed by a number of scientists, including Kühn [1] and Cheng [2]. Kühn used higher-order stream function theory to assess extreme regular waves. Cheng used a random linear wave model to study extreme responses during normal operation. A study of fatigue loads on wind power plants during normal operation has been made by Veldkamp and van der Tempel [3].

METHOD

For the wave load calculation, a number of realizations of the elevation are made with Pierson-Moskowitz spectra giving the statistical properties of the sea surface elevation. If H_{max} of the second-order realization is greater than 0.78 h, which is the depth-breaking limit for the waves [4, 5], the realization is discarded and another realization is chosen. The phase angles from the chosen realization are used to calculate the corresponding velocity potential.

To avoid unrealistically large local wave steepness with associated velocities and accelerations, which otherwise would result in non-physical forces, a cut-off of the spectrum is done. The maximum value for the angular frequency ω is taken as

$$\omega_{\max} = \sqrt{\frac{2g}{0.95H_{m0}}} \qquad \textbf{Eq. 1}$$

where H_{m0} is the significant wave height and g is the acceleration of gravity [6].

There are several implementations of a cut-off at the high frequency end of the spectrum. Equation 1 is from the work of Nestegård and Stokka [7] as it is used in the PhD-thesis by Brodtkorb [6]. It gives, with $n = 3.7$, a similar result to the cut-off suggested by Massel [5], who uses $\omega_{max} = n\omega_p$, where ω_p is the peak frequency of the spectrum and $n > 3$. As the second-order solution adds energy around the double peak frequency the cut-off has

to be sufficiently high in order not to exclude energy at higher frequencies. The cut-off should also be high enough to include the eigen-frequency of the structure. For the chosen wind turbine the eigen-frequency is 0.32 Hz. This frequency is included for all wind speeds up to 22 m/s. The relatively low cut-off at 22 m/s and 24 m/s is not a problem, as there is very little energy at those frequencies and the aerodynamic damping of the system is high. However, the important thing is to use a low enough cut-off frequency in order to avoid non-physical forces.

The Pierson-Moskowitz spectrum is given as

$$S_{PM} = \frac{\alpha g^2}{(2\pi)^4} f^{-5} e^{-0.74\left(\frac{g}{2\pi U_{19.5m}}/f\right)^4} \quad \textbf{Eq. 2}$$

where $\alpha = 0.0081$, f is the frequency and $U_{19.5m}$ is the wind speed at 19.5 meters above sea level [5].

In principle a complete 3-D Navier-Stokes simulation, with free water surface, or a second-order diffraction model could be used for the purpose of calculating the wave force on the structure. However, the goal is to make many effective calculations, and as the incident wave can be considered practically undisturbed by the presence of the monopile, $D < 0.2\ \lambda$, and the viscous effects are small, $H < 10\ D$ [8], 3-D simulations would not give more information. In the above section λ is the wavelength and H is the wave height.

Second-order realization of waves

The method for calculating the non-linear waves is treated in *e.g.* Sharma and Dean [9], Hudspeth and Chen [10] and A. H. Madsen [11]. If the difference frequencies are discarded the solution to the linear problem can be expressed by the Fourier series

$$\Phi^{(1)}(x,z,t) = -i\sum_{m=0}^{N} F(m)\frac{g}{\omega_m}\frac{\cosh\left[k_m(z+h)\right]}{\cosh(k_m h)}\exp i(\omega_m t - k_m x) \quad \textbf{Eq. 3}$$

for the velocity potential, Φ, and

$$\eta^{(1)}(x,t) = \sum_{m=0}^{N} F(m)\exp i(\omega_m t - k_m x)\,, \quad \textbf{Eq. 4}$$

for the surface elevation, η, where the wave number k is given by the dispersion relation

$$\omega_m^2 = g k_m \tanh k_m h\,, \quad \textbf{Eq. 5}$$

i is the imaginary unit, ω is the angular frequency, g is the acceleration of gravity and h is the water depth. The superscript (1) is the perturbation ordering parameter. For the non-linear solution the first, linear, and the second order contributions to the velocity potential and surface elevation are added to give the total, non-linear, solution. The solution to the second-order problem is expressed by

$$\Phi^{(2)}(x,z,t) = -i\sum_{n=0}^{N}\sum_{m=0}^{N}\frac{F(n)F(m)}{2}D(\omega_n,\omega_m)\frac{\cosh\left[(k_n+k_m)(z+h)\right]}{\cosh\left[(k_n+k_m)h\right]}\exp i\left[(\omega_n+\omega_m)t-(k_n+k_m)x\right] \quad \textbf{Eq. 6}$$

and

$$\eta^{(2)}(x,t) = \sum_{n=0}^{N}\sum_{m=0}^{N}\frac{F(n)F(m)}{4g}H(\omega_n,\omega_m)\exp i\left[(\omega_n+\omega_m)t-(k_n+k_m)x\right], \quad \textbf{Eq. 7}$$

where

$$D(\omega_n,\omega_m)=\frac{2(\omega_n+\omega_m)\left[g^2k_nk_m-(\omega_n\omega_m)^2\right]-\omega_n\omega_m(\omega_n^3+\omega_m^3)+g^2(\omega_mk_n^2+\omega_nk_m^2)}{2\omega_n\omega_m\left[(\omega_n+\omega_m)^2-g(k_n+k_m)\tanh(k_n+k_m)h\right]} \quad \textbf{Eq. 8}$$

and

$$H(\omega_n,\omega_m)=2(\omega_n+\omega_m)D(\omega_n,\omega_m)-\frac{g^2k_nk_m}{\omega_n\omega_m}+(\omega_n+\omega_m)^2-\omega_n\omega_m\,. \quad \textbf{Eq. 9}$$

The complex amplitude *F(n)* is given by

$$F(n)=\sqrt{2S(\omega_n)\Delta\omega}\exp(-i\varepsilon_n) \quad \textbf{Eq. 10}$$

where S is the variance density spectrum, for example S_{PM}, $\Delta\omega$ is the frequency resolution, and ε is a random phase angle distributed between 0 and 2 π. The use of the variance density spectrum for calculating the complex amplitudes retains the statistical properties of the sea. Equations 3 through 10 are valid for finite depth and small waves [9]. *

Calculation of water velocities

The water particle velocities are given by the spatial derivative of the velocity potential Φ as

$$u=-\Phi_x\ ,\ w=-\Phi_z \quad \textbf{Eq. 11}$$

where the subscript denotes partial differentiation.

As the force along the monopile is to be calculated to the free surface the water particle velocities to the free surface are needed. In order to prevent the calculated velocities above the still water level from becoming unrealistically high two methods are used. For the first method an approximation to the wave particle kinematics above still water level is implemented by a Taylor expansion to the first order around $z = 0$ [7]

$$u(x,z,t)=\Phi_x\big|_{z=0}+\Phi_{xz}\big|_{z=0}\,z\,. \quad \textbf{Eq. 12}$$

The second method is Wheeler stretching [14], were the velocities are stretched from the still water surface to the instantaneous free surface. These approximations are used for both the linear and non-linear realizations.

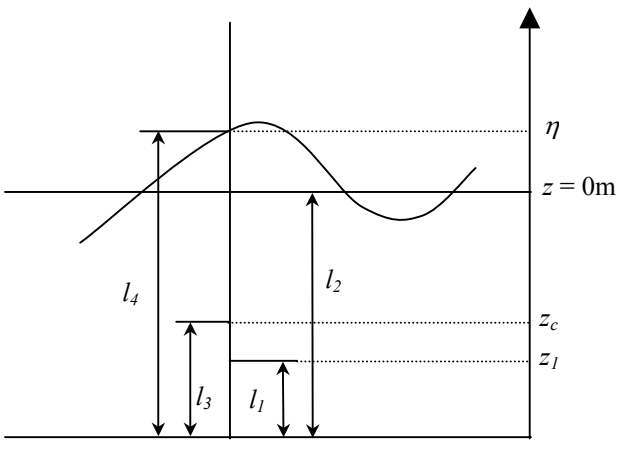

Figure 2. *Wheeler stretching*

For the Wheeler stretching the velocities are calculated in fixed grid points between the bottom and the still water level. These velocities are then applied at a grid, which is stretched to the free water surface, η, according to the relation $l_1/l_2 = l_3/l_4$. The new stretched coordinate z_c is calculated as

$$z_c=\frac{z_1\eta}{h}+z_1+\eta \quad \textbf{Eq. 13}$$

where z_1 is the original grid coordinate. After the stretching the results are interpolated to a grid which is fixed in time in order to facilitate the export of the forces to HawC. See Fig. 2.

* As the basic references [10, 12] were interpreted in a previous paper [13] there seems to be a factor ½ missing in Eqs. 6 and 7, which is corrected here and the paper by Sharma and Dean is used as reference instead [9].

Computation of structural forces and moments

The incident wave is assumed to be undisturbed by the presence of the monopile. This is valid for all practical purposes when the ratio of structure diameter to wavelength is small [8]. The usually accepted criterion is that this ratio should be less than 0.2, but there is no sharp limit. For the mildest sea state used here, a wind speed of 6 m/s at hub height, the lengths of the most frequent waves are 30 m, so the ratio is around 0.2. For the next sea state, at 8 m/s, the ratio is 0.1, and it decreases for higher winds.

The undisturbed incident wave can thus be used to calculate the wave force P and resulting moment M on the monopile in combination with Morison's equation, integrating along the monopile and lumping the loads in nodes for the response calculation. The integration is carried out to the free surface elevation in order to take into account that forces only act on the submerged part of the monopile.

$$P = \frac{1}{2}\rho C_D D \int_{-h}^{\eta} u|u|dz + \rho \frac{\pi D^2}{4} C_M \int_{-h}^{\eta} u_t dz \qquad \textbf{Eq. 14}$$

and

$$M = \frac{1}{2}\rho C_D D \int_{-h}^{\eta} u|u|(z+h)dz + \rho \frac{\pi D^2}{4} C_M \int_{-h}^{\eta} u_t (z+h)dz \; . \qquad \textbf{Eq. 15}$$

Here C_D is the drag coefficient, C_M is the inertia coefficient, ρ is the water density and D is the diameter of the monopile [15]. Figure 1 depicts the monopile. The choice of C_D and C_M in this study is not critical as the focus is on comparing different wave models. The monopile is considered to be stiff and therefore its displacement velocity and acceleration are neglected.

Fatigue calculations

To study the fatigue load effects, a generic 5 MW pitch-controlled wind turbine is used. It has a tower diameter of 6 meters at sea level, a rotor diameter of 110 meters and a hub height of 80 meters from the sea level. The turbine has a design life of twenty years.

The structure response calculations were carried out using the program HawC [16-18] developed at Risø, for mean wind speeds ranging from 6 m/s to 24 m/s with a 2 m/s increment. The wind speeds, at hub height of the wind turbine, were recalculated, with a wind shear power law factor of 0.2 [19], to the wind speed at a height of 19.5 m above sea level and used as input to the Pierson-Moskowitz spectra. For these wind speeds the wind turbine is in production. The wind and waves are in line with each other, and act in the same direction.

Six sets of response calculations were made. Within each set five different fatigue calculations, with the same realization of the turbulent wind field, were made. The five fatigue calculations were carried out with linear waves, with non-linear waves, for the Taylor extrapolation and the Wheeler stretching respectively, and without wave loading. For the realization of the wave loads, the same phase angles were used for both the linear and non-linear cases within each set of simulations for the respective mean wind speeds. Reusing the realizations of the turbulent wind field keeps the influence of lack of ergodicity at a minimum. The effect of including non-linearities could in some cases be so small that it would potentially vanish in statistical noise if different realizations of the stochastic wind speed process were used.

The influence of the wave loads on the response of the blades of the turbine is believed to be small, and with this in mind only the supporting structure is studied. Only the moment around the axis perpendicular to the wave propagation (i.e. parallel to the wave crests) is studied, as this is believed to be clearly indicative of the difference in effect between the wave loads. The fatigue calculations are made at mud level for the bending moment *My* in the tower. For the calculation of the accumulated fatigue damage, the moment is recalculated to stress levels.

The stress for a cylinder can be calculated as

$$\sigma = \frac{My}{Wy} \qquad \textbf{Eq. 16}$$

where

$$Wy = \frac{\pi}{4} D^2 t \, , \qquad \textbf{Eq. 17}$$

t is the thickness of the cylinder and D is the outer diameter of the cylinder.

The stress range distribution is the number of stress (or moment) cycles that take place within a specific stress (or moment) range. See *e.g.* Fig. 3. The distribution is obtained using rain flow counting for the calculated ten-minute structural response time series.

To account for the entire life span of the wind turbine, the mean wind speeds are considered to be Rayleigh-distributed with an average value of 10 m/s. The distribution is used to give the number of hours for which each wind speed occurs during the planned life, of typically twenty years, of the wind turbine. Knowing the distribution of mean wind speeds during the life span of the wind turbine, and the load history for the ten ten-minute response calculations of the structure, the total accumulated damage can be obtained.

The accumulated damage D_{acc} can be predicted as follows:

$$D_{acc} = \sum_{i=1}^{k} \frac{\Delta nc(SR_i)}{\Delta NC(SR_i)} \qquad \textbf{Eq. 18}$$

where Δnc is the number of cycles at the stress range SR in the lifetime of the structure. ΔNC is the number of cycles to failure at this stress range.

This is the Palmgren-Miner rule, and it should be noted that the damages for different stress cycles are considered to be independent of each other, *i.e.* a stress cycle induces the same damage regardless of when in the life span of the structure it occurs. This is reasonable for metallic materials used for typical monopiles. Though not entirely correct, the deviation of the mean load from zero is neglected in the present fatigue study. This may be a bit misleading when the results are studied, as the wind load appears to be much smaller than the wave load. This is not the case; it is the deviation around the mean value that is smaller for the wind load compared to the wave load.

The number of stress cycles to failure can be obtained from Wöhler curves, for the material in question, as

$$NC = K \cdot SR^{-m} \qquad \textbf{Eq. 19}$$

in which K and m are empirical material constants.

For the accumulated damage, two methods have been used with a linear and a bi-linear Wöhler curve (the curves will be linear in a log-log plot). The first method is defined by Eq. 19 with $m = 3$ and $\log10(K) = 11.851$, and all the ratios in the sum in Eq. 18 are counted. Two expressions like Eq. 19 define the bi-linear Wöhler curve. For stresses higher than 52 MPa, the line is defined by Eq. 19 with $m = 3$ and $\log10(K) = 11.851$, and otherwise by $m = 5$ and $\log10(K) = 15.286$. For stress levels of less than 29 MPa there is no contribution to the summation in Eq. 18 [20]. The results are very sensitive to the choice of Wöhler curve. However, the linear Wöhler curve can very well be used when comparing the different wave loads as the focus is on the difference in fatigue damage between the different wave models.

RESULTS

The fatigue is studied for the bending moment at mud level, as this is representative for the most important combination of wind and wave loads in design of monopiles against fatigue, and has the maximum contribution from the waves. The results from the fatigue calculations from the six different sets of calculations were averaged to obtain mean stress range distribution plots (Figs. 3 and 4). The results are summarized in Tables 1 to 4. Tables 1 and 2 contain the accumulated fatigue damage for the whole lifetime of twenty years for the structure, for the linear and the bi-linear Wöhler curve respectively. The bottom rows show the ratio of non-linear to linear accumulated fatigue damage. Tables 3 and 4 show the averaged relative contribution to fatigue damage per wind speed for the whole lifetime of the structure, Taylor extrapolation and Wheeler stretching respectively.

There is surprisingly little contribution to the accumulated fatigue damage from the wind load. This can be explained by the fact that there are more load cycles at high stress ranges for the cases with wave loads than for the ones without wave loads. See Figs. 3 and 4.

For the linear Wöhler curve the Taylor expansion gives an averaged accumulated damage for the non-linear wave load which is 12% larger than for the linear wave load. For the Wheeler stretching the same result is 7%. The difference between the linear and non-linear wave load increases dramatically if the bi-linear Wöhler curve

is used. The non-linear wave load is 80% larger than the linear for the Taylor extrapolation and 51% larger for the Wheeler stretching.

Taylor expansion								**Wheeler stretching**							
LW	1	2	3	4	5	6	**Mean**	**LW**	1	2	3	4	5	6	**Mean**
Linear	0.52	0.50	0.48	0.46	0.52	0.50	**0.50**	Linear	0.45	0.46	0.43	0.41	0.46	0.47	**0.45**
Non-linear	0.60	0.54	0.53	0.51	0.59	0.56	**0.55**	Non-linear	0.49	0.48	0.46	0.43	0.53	0.48	**0.48**
No wave	0.08	0.09	0.07	0.07	0.09	0.09	**0.08**	No Wave	0.08	0.09	0.07	0.07	0.09	0.09	**0.08**
NL/L	1.17	1.08	1.10	1.11	1.13	1.11	**1.12**	NL/L	1.10	1.04	1.09	1.04	1.13	1.01	**1.07**

Table 1. *Accumulated fatigue damage for the whole lifetime of the structure. LW stands for a calculation with a linear Wöhler curve with m = 3. NL/L is the ratio of non-linear to linear damage.*

Taylor expansion								**Wheeler stretching**							
BLW	1	2	3	4	5	6	**Mean**	**BLW**	1	2	3	4	5	6	**Mean**
Linear	0.09	0.05	0.06	0.04	0.05	0.05	**0.06**	Linear	0.06	0.03	0.03	0.02	0.03	0.04	**0.03**
Non-linear	0.17	0.08	0.08	0.09	0.11	0.08	**0.10**	Non-linear	0.08	0.05	0.05	0.03	0.07	0.04	**0.05**
No wave	0	0	0	0	0	0	**0**	No Wave	0	0	0	0	0	0	**0**
NL/L	1.80	1.63	1.46	2.27	2.02	1.81	**1.80**	NL/L	1.36	1.60	1.62	1.51	2.26	0.97	**1.51**

Table 2. *Accumulated fatigue damage for the whole lifetime of the structure. BLW stands for a bi-linear Wöhler curve according to Eurocode 3 [20]. NL/L is the ratio of non-linear to linear damage.*

As the focus of the study is on the difference between a linear and a non-linear wave model and the difference between two different methods of extrapolating the water particle velocities to the free surface, the averaged relative contribution to fatigue damage per wind speed has been listed in Table 3 and 4. Another motive to study the relative damage per wind speed is to get an idea of which wind speed causes the most damage, in this case 16 m/s. Table 3 and 4 contains results calculated using a linear Wöhler curve with $m = 3$. The high relative fatigue damage at 6 m/s, for the cases without wave loads, is the result of an excitation by the blade passing frequency, at the eigen frequency of the support structure. Table 3 and 4 also shows a clear trend that the fatigue contribution shifts from lower to higher mean wind speeds when one goes from a linear to a non-linear wave model. This trend is explained by the fact that when applying the non-linear model, the wave loads at the crests of the waves are enhanced. When the non-linearity is higher, the resulting wave height will be increased, and in turn be larger at higher mean wind speeds. This is true for both the Taylor extrapolation and the Wheeler stretching, but the effect is more pronounced for the Taylor extrapolation.

Taylor extrapolation										
Windspeed	6m/s	8m/s	10m/s	12m/s	14m/s	16m/s	18m/s	20m/s	22m/s	24m/s
Linear	4.83	9.32	10.10	11.58	16.95	**21.16**	12.24	6.41	4.57	2.82
Non-linear	4.29	8.18	8.77	10.05	14.75	**19.01**	12.09	7.73	7.24	7.89
No wave	6.22	1.51	1.79	2.01	14.36	**36.01**	17.59	9.80	6.74	3.97

Table 3. *Relative contribution to fatigue damage per wind speed for the whole lifetime of the structure for m = 3. Maxima are indicated in bold letters.*

Wheeler stretching										
Windspeed	6m/s	8m/s	10m/s	12m/s	14m/s	16m/s	18m/s	20m/s	22m/s	24m/s
Linear	5.38	10.23	10.92	12.00	15.88	**21.71**	11.43	6.03	4.08	2.34
Non-linear	5.08	9.54	10.10	11.05	15.46	**21.19**	11.57	6.67	5.18	4.15
No wave	6.22	1.51	1.79	2.01	14.36	**36.01**	17.59	9.80	6.74	3.97

Table 4. *Relative contribution to fatigue damage per wind speed for the whole lifetime of the structure for m = 3. Maxima are indicated in bold letters.*

Studying the average stress range distribution for the whole life of the structure, Figs. 3 an 4, it is not evident that the non-linear cases should give a higher contribution to the fatigue load. However, for the non-linear cases there is a small number of stress cycles at high stress ranges, and due to the power law in Eq. 19 they contribute greatly to the accumulated fatigue damage. The small number of stress cycles at high stresses can just barely be seen in the zoom of the plots. For the bi-linear case, only values higher than 29 MPa are counted and this makes the accumulated fatigue damage sensitive to the number of stress cycles at values higher than 29 MPa.

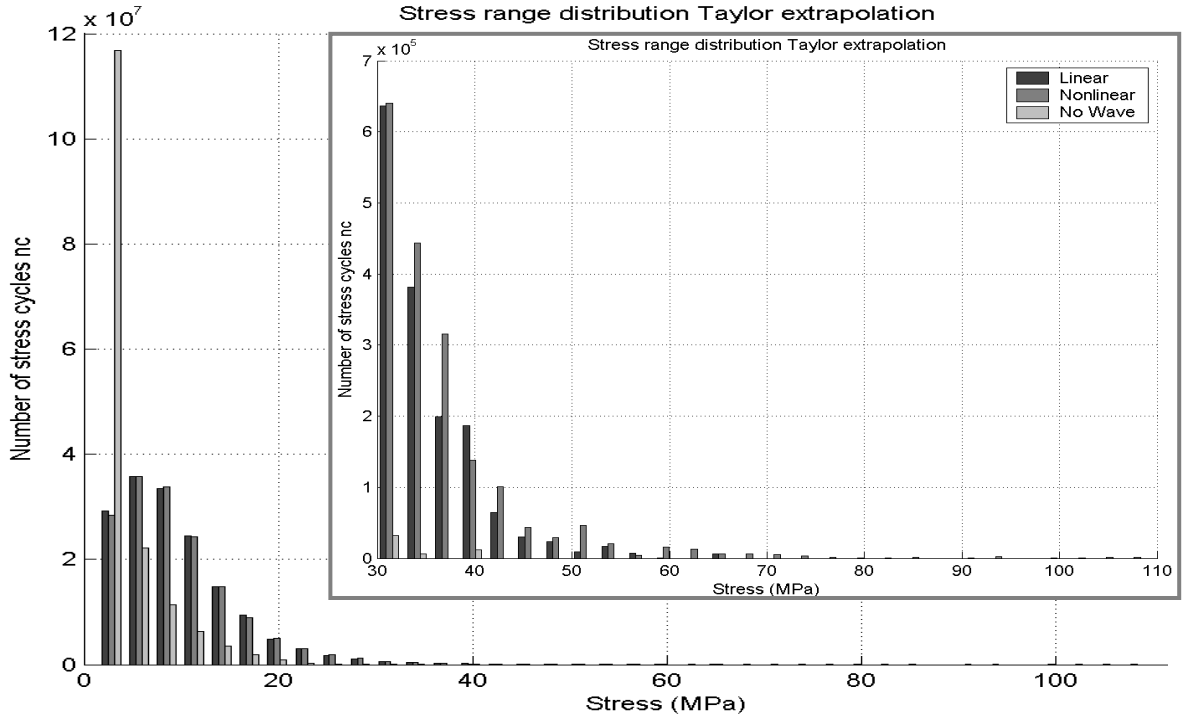

Figure 3. *Taylor extrapolation. Lifetime average stress range distribution for all the six sets of calculations. The inserted plot shows a zoom of values above 30 MPa. The non-linear simulations give stress cycles at high stresses. There is little contribution from the case without wave load at stress levels above 30 MPa.*

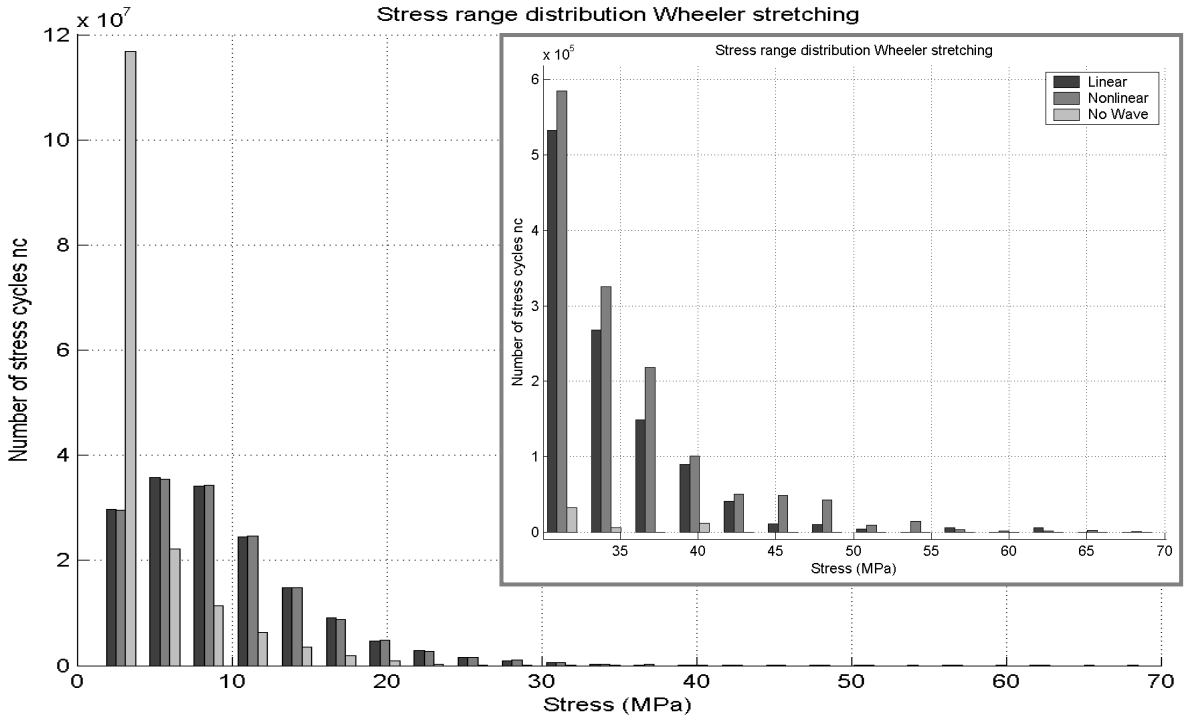

Figure 4. *Wheeler stretching. Lifetime average stress range distribution for all the six sets of calculations. The inserted plot shows a zoom of values above 30 MPa. The non-linear simulations give stress cycles at high stresses. There is little contribution from the case without wave load at stress levels above 30 MPa.*

CONCLUDING REMARKS

It can be seen, when studying the support structure at mud level, that the wave loads contribute significantly to the accumulated fatigue damage. The contribution from the wave load is larger than the contribution from the wind load. The difference between the linear and non-linear wave model is 12% for the Taylor extrapolation and 7% for the Wheeler stretching if a linear Wöhler curve with $m = 3$ is used. For the linear wave model the Taylor extrapolation method is 11% higher than the Wheeler stretching and for the non-linear case the difference is 15%, still using a linear Wöhler curve with $m = 3$. The results are sensitive to the relatively few high stress levels, suggesting that care should be taken to use a wave model that reproduces both the particle kinematics underneath high and steep waves, and the wave height distribution correctly.

As the total simulation time for the load calculation is a few times ten minutes, the statistical uncertainty in the assessment of the number and magnitude of the few high stress levels is indeed large. Multiplying the structural loads for a specific wind speed with the duration of that wind speed over the life of the wind turbine may significantly influence the uncertainty of fatigue life consumption, this is the case in the present study. Regardless of the method chosen to calculate the time-series of the irregular waves, there is a need for more or longer time series for the waves if the number of stress cycles for high stresses is to be calculated correctly.

This is more important if the bi-linear Wöhler curve is used. When stress cycles below 29 MPa are excluded, the total fatigue damage becomes sensitive to variations in the stress ranges above 29 MPa. It can be seen in Table 2 that there are large differences in the total fatigue damage between the six sets of wave loads. On the other hand, the total damage is decreased.

The research by Stansell [21] shows that the wave height distribution in deep waters deviates from the Rayleigh distribution. Stansell has studied the distribution of freak wave heights measured in the North Sea, and has found that the Rayleigh distribution under-predicts the probability of occurrence for such waves. This suggests that the linear model used in our study is not describing the wave height distribution sufficiently well. The linear wave elevation is Gaussian and the wave heights are Rayleigh distributed. The non-linear model is non-Gaussian but the validity of the model needs to be investigated.

For the non-linear case in Table 3, the Taylor extrapolation, the contribution at 24 m/s is increased compared to the one at 22 m/s. An explanation for this could be that the wave breaking criterion of 0.78 h used in the present paper is high. A breaking criterion of 0.55 h instead is proposed in [5]. Had this more restrictive breaking criterion been employed, the wave loads at high mean wind speeds would of course have been less, thus reducing the likelihood that a high contribution from the 24 m/s time series would occur. A discussion of the largest wave height in water of constant depth can be found in [5]. The limiting value for H_{max} of 0.55 h is found to apply to shallow water waves. This is a more restrictive value than the breaker height limit 0.78 h for mildly shoaling bottoms used in the calculation above. The implication is that for shoaling cases 0.78 h should be used, and for vast shallows 0.55 h may be more accurate but less conservative. For the same case when Wheeler stretching is used the value at 24 m/s is lower than at 22 m/s. This is due to the reduced water particle velocities at the wave crests for the Wheeler stretching compared to the Taylor extrapolation.

It can be seen that the choice of method for the extrapolation of the wave kinematics to the free surface above still water level, as well as the distribution of wave heights, is relevant to the fatigue loads on the structure. The Wheeler stretching gives lower velocities at the crests than the Taylor expansion. This reduces the fatigue load for both the linear and non-linear wave loads. The difference between the linear and non-linear cases is smaller if Wheeler stretching is used. The Wheeler stretching can, however, underestimate the particle kinematics for steep waves. In fact the velocity profile would be somewhere in between the Taylor extrapolation, which would overestimate the velocity under the wave crest, and the Wheeler stretching, which underestimates the velocity under the wave crest. This has been studied by Smith and Swan [22] and they suggest that a model taking both the non-linearities and the unsteadiness of the extreme wave event into account should be used. In doing so, they use Fourier series solutions to the wave dynamics incorporating non-linear wave-wave interactions and the rapid redistribution of energy within the frequency domain. Their results rely on either a measurement or an exact calculation of the wave elevation. However, their results show very good agreement with measurements and exact numerical calculations of the wave kinematics.

The fatigue load calculation is sensitive to the number of high stress ranges, and it is important that both the wave height distribution and the kinematics of the waves are calculated correctly. The work by Smith and Swan [22] and Stansell [21] clearly show that these are important areas of study.

ACKNOWLEDGMENTS

For the first author the financial support given by the Swedish Energy Agency is gratefully acknowledged. For the second and third authors the financial support of EU under contract number ENK5-CT-2000-00322 (RECOFF) is gratefully acknowledged.

REFERENCES

1. Kühn, M., *Dynamics and Design Optimisation of Offshore Wind Energy Conversion Systems*, in *Wind Energy Research Institute*. 2001, Delft University: Delft.
2. Cheng, P.W., *A Reliabillity Based Design Methodology for Extreme Responses of Offshore Wind Turbines*, in *Wind Energy Research Institute*. 2002, Delft University: Delft.
3. Veldkamp, H.F. and J. Van Der Tempel, *Influence of wave modelling on the prediction of fatigue for offshore wind turbines.* Wind Energy, 2005. **8**(1): p. 49-65.
4. *Shore Protection Manual*. Vol. 1. 1977, Fort Belvoir: U.S. Army Coastal Engineering Research Center.
5. Massel, S.R., *Ocean Surface Waves: Their Physics and Prediction*. Advanced Series on Ocean Engineering. 1996, Singapore: World Scientific Publishing.
6. Brodtkorb, P.A., *The Probability of Occurrence of Dangerous Wave Situations at Sea*. 2004, Norwegian University of Science and Technology: Trondheim. p. 146-154.
7. Nestegård, A. and T. Stokka, *Third-order random wave model*. in *5th 1995 International Offshore and Polar Engineering Conference*. 1995. Hague, Neth: Int Soc of Offshore and Polar Engineerns (ISOPE),Golden,CO,USA.
8. Faltinsen, O.M., *Sea loads on ships and offshore structures*. Cambridge Ocean Technology Series. 1990, New York: The Press Syndicate of the University of Cambridge.
9. Sharma, J.N. and R.G. Dean, *Second-Order Directional Seas and Associated Wave Forces.* Society of Petroleum Engineers Journal, 1981. **21**(1): p. 129-140.
10. Hudspeth, R.T. and M.-C. Chen, *Digital Simulation of Nonlinear Random Waves.* Journal of the Waterway, Port, Coastal and Ocean Division, Proceedings of the American Society of Civil Engineers, 1979. **105**(1 Feb): p. 67-85.
11. Madsen, A.H., *A quadratic theory for the fatigue life estimation of offshore structures.* Applied Ocean Research, 1987. **9**(2): p. 67-80.
12. Machado, U.B., *Probability density functions for non-linear random waves and responses.* Ocean Engineering, 2003. **30**(8): p. 1027-1050.
13. Trumars, J.M.V., J.O. Jonsson, and L. Bergdahl, *Extreme non-linear wave forces on a monopile in shallow water*. in *22nd International Conference on Offshore Mechanics and Arctic Engineering; Materials Technology Ocean Engineering Polar and Arctic Sciences and Technology Workshops, Jun 8-13 2001*. 2003. Cancun, Mexico: American Society of Mechanical Engineers.
14. Wheeler, J.D., *Method for Calculating Forces Produced by Irregular Waves.* Journal of Petroleum Technology, 1970. **22**(3): p. 359-67.
15. Sarpkaya, T. and M. Isaacson, *Mechanics of wave forces on offshore structures*. 1981, New York: Van Nostrand Reinhold Company Inc.
16. Petersen, J.T., *Kinematically Nonlinear Finite Element Model of a Horizontal Axis Wind Turbine. Part 1: Mathematical Model and Results*. 1990, Risø National Laboratory: Denmark.
17. Petersen, J.T., *Kinematically Nonlinear Finite Element Model of a Horizontal Axis Wind Turbine. Part 2: Supplement. Inertia Matrices and Aerodynamic Model*. 1990, Risø National Laboratory: Denmark.
18. Petersen, J.T., *The Aeroelastic Code HawC- Model and Comparisons*. in *28th IEA Experts Meeting: 'The State of the Art of Aeroelastic Codes'*. 1996. DTU, Lyngby, Denmark.
19. *International Standard: Wind turbine generator systems, Part 1: Safety requirements, (IEC 61400-1:1999(E)), second edition*. 1999. p. 21.
20. *Eurocode No. 3: Design of steel structures, Part 1-1: General rules and rules for buildings (ENV 1993-1-1)*. 1993. p. 214-237.
21. Stansell, P., *Distributions of freak wave heights measured in the North Sea.* Applied Ocean Research, 2004. **26**(1-2): p. 35-48.
22. Smith, S.F. and C. Swan, *Extreme two-dimensional water waves: An assessment of potential design solutions.* Ocean Engineering, 2002. **29**(4): p. 387-416.